

# Crazing as a Method for Preparation of Polymer Blends

L. M. Yarysheva, E. G. Rukhlya, A. Yu. Yarysheva, A. L. Volynskii, and N. F. Bakeev

*Department of Chemistry, Moscow State University, Moscow, 119991 Russia*  
*e-mail: alyonusha@gmail.com, yarishev@gmail.com, volynskii@gmail.com*

Received November 29, 2010; in final form, April 6, 2011

**Abstract**—Publications on the development of a new universal method for the preparation of polymer–polymer blends are reviewed. This approach is based on the phenomenon of solvent crazing, which comes into play in the tensile drawing of polymers in the presence of adsorption-active liquid media. It is important that solvent crazing is accompanied by the development of a unique fibillar–porous structure, in which the dimensions of craze pores and fibrils do not exceed several tens of nanometers. Two approaches to the preparation of the polymer–polymer blends are described. According to the first approach, the nanoporous structure of the solvent-crazed polymer is filled with the monomer, and its further in situ polymerization results in the polymer–polymer blends. The second approach has been recently advanced by the authors of this publication; it involves direct penetration of macromolecules into the formed fibillar–porous structure of the solvent-crazed polymer. Both approaches are capable of producing diverse polymeric blends with a high degree of mutual dispersion of the components. The above materials are shown to be characterized by specific mechanical, electrical, and adsorption properties, which are due to the unique fibillar–porous structure of the solvent-crazed polymer. The composition, structure, and properties of the prepared blends are controlled by the mechanism of solvent crazing and by the deformation conditions of the initial polymer. Several aspects of the practical application of the polymer blends prepared via the mechanism of solvent crazing in adsorption-active liquid media are reviewed.

**Keywords:** solvent-crazed polymers; polymer blends; structure of polymer blends; electrical, adsorption, and mechanical properties of polymer blends.

**DOI:** 10.1134/S2079978011030046

## CONTENTS

1. Introduction
2. Solvent Crazing as a Method for Preparing Polymers with Nanoscale Porosity
3. Peculiarities of the Formation of Polymer–Polymer Blends Based on Polymers Deformed in Liquid Media by the Mechanism of Solvent Crazing
  - 3.1. *Peculiarities of the Formation of Polymer–Polymer Blends by in situ Polymerization in a Solvent-Crazed Polymer Matrix*
  - 3.2. *Direct Introduction of the Second Polymer Component into the Polymer Deformed by the Mechanism of Solvent Crazing*
4. Physicomechanical Properties of Polymer Blends Obtained by Solvent Crazing
  - 4.1. *Mechanical Properties of Polymer Blends Obtained by In Situ Polymerization in a Solvent-Crazed Polymer Matrix*
  - 4.2. *Adsorption Properties of Polymer–Polymer Nanocomposites Obtained by In Situ Polymerization in a Solvent-Crazed Polymer Matrix*
  - 4.3. *Electrically Conductive Polymer Blends Obtained by In Situ Polymerization in a Solvent-Crazed Polymer Matrix*
  - 4.4. *Prolonged Release of a High-Viscosity Component from the Structure of the Solvent-Crazed Polymer*

## 1. INTRODUCTION

In recent years, research fields related to obtaining multicomponent multiphase polymer systems have been rapidly developed. The main obstacle hindering progress in this area is the thermodynamic incompatibility of most polymers with each other, associated with small values of the entropy of mixing [1]. As a result, mixed polymers fall apart from one another into extended phases with a poor mutual adhesion,

which significantly affects the properties of the resulting compositions. To overcome the issues associated with the poor compatibility of polymers, a productive approach is used involving the formation of polymer–polymer nanocomposites, that is, the creation of stable multiphase systems with a high level of mutual dispersion. Nanocomposites of this kind can be obtained through the simultaneous or sequential polymerization of two monomers under conditions excluding their copolymerization. This approach allows one to achieve a high mutual dispersion of polymer components in the final product. This method has been known for a long time and has been developed for the so-called interpenetrating polymer networks (IPNs) [2]. These polymer–polymer blends are synthesized through the combination of two or more monomers and their subsequent independent polymerization. In this case, the phase separation occurs in the system during polymerization; however, it does not lead to a layering of the system under such conditions. As a result, IPNs are two-phase systems with a high level of mutual dispersion of the components occurring in contact with each other.

There are two main ways of obtaining IPNs:

1. Simultaneous IPNs (systems obtained by simultaneous polymerization of two or more monomers);
2. Sequential IPNs (systems obtained by the swelling of monomer **2** in the final network of polymer **1**, followed by its in situ polymerization).

The main peculiarities of obtaining IPNs are summarized in Sperling's monograph [2].

Regarding the subject of this review, it is important to note that the vast majority of IPNs are typical nanosystems. Indeed, the domain sizes of polymer **2** in the network of polymer **1** ( $D_2$ ) can be expressed as [3]:

$$D_2 = (2\gamma W_2)/RTv_1\{1/(1 - W_2)^{2/3} - 1/2\}, \quad (1)$$

where  $W_2$  is the mass fraction of component **2**,  $\gamma$  is the interfacial energy,  $v_1$  is the effective number of moles of cross-linked polymer chains in the network of polymer **1**,  $R$  is a universal gas constant, and  $T$  is absolute temperature. Equation (1) has been subjected to numerous experimental tests using direct microscopic measurements of phase domains in the IPNs.

It was shown that, in most cases, the size of phase domains calculated from Eq. (1) and identified by electron microscopy corresponded well to each other. Moreover, for IPNs based on styrene–butadiene rubber and polystyrene (PS), for example, these dimensions are from 48 to 150 nm depending on the composition and degree of cross-linking [3]; therefore, these systems can be attributed to typical nanocomposites. The calculations for IPNs based on castor oil–urethane–PS give the dimensions of phase domains from 25 to 55 nm, which is fully confirmed by the data of electron microscopy [4]. Similar results were obtained in [5–8]. Even a homo IPN on the basis of PS (these systems are obtained by the swelling of cross-linked PS in styrene followed by in situ polymerization) also demonstrates the presence of domains with dimensions of 6–10 nm [9]. According to differential scanning calorimetry, small-angle X-ray scattering, and other methods, the size of aggregates in polyethylene oxide in semi-interpenetrating networks based on cross-linked polymethacrylate was approximately 10 nm [10].

In recent years, IPNs have often been received in the form of multiphase nanogels suitable for solving many important practical problems, such as modulation of light [11], detection of hemoglobin in aqueous solutions [12], prolonged release of low-molecular-weight ligands to the environment [13], and others [14, 15]. Moreover, the principle of obtaining IPNs is used to create conventional nanocomposites: so-called organic–inorganic hybrid polymer materials [16–18].

Thus, there is a widely used method for obtaining polymer–polymer nanocomposites through the implementation of two independently occurring processes of polymer synthesis, accompanied by the phase separation of polymer components.

At the same time, there is a fundamentally different approach to the creation of polymer–polymer nanocomposites. In the most general form, this approach involves creating a nanoporous polymer matrix, followed by filling the formed pores with the second polymer component. With this approach, the phase nonhomogeneity of the components does not arise in the course of polymerization but is laid at the stage when the nanoporosity polymer matrix appears. This method is widely used for the modification of polymer membranes. For example, to impart hydrophilicity and improve the separation selectivity with respect to water, new composite membranes were obtained based on porous polyethylene films and cross-linked polyacrylic acid [19]. In the same microporous polyethylene matrices, the polymerization of conductive polymers was carried out in [20].

The crazing of polymers in liquid media is a universal method of imparting polymer films and fibers with nanoscopic porosity [21, 22]. In this regard, the use of nanoporous solvent-crazed polymers appears promising, in terms of creating new types of polymer–polymer blends with a high level of dispersion of components.

The purpose of this review is to analyze the data related to the method of obtaining polymer–polymer blends using solvent-crazed polymers and to demonstrate some of their properties.

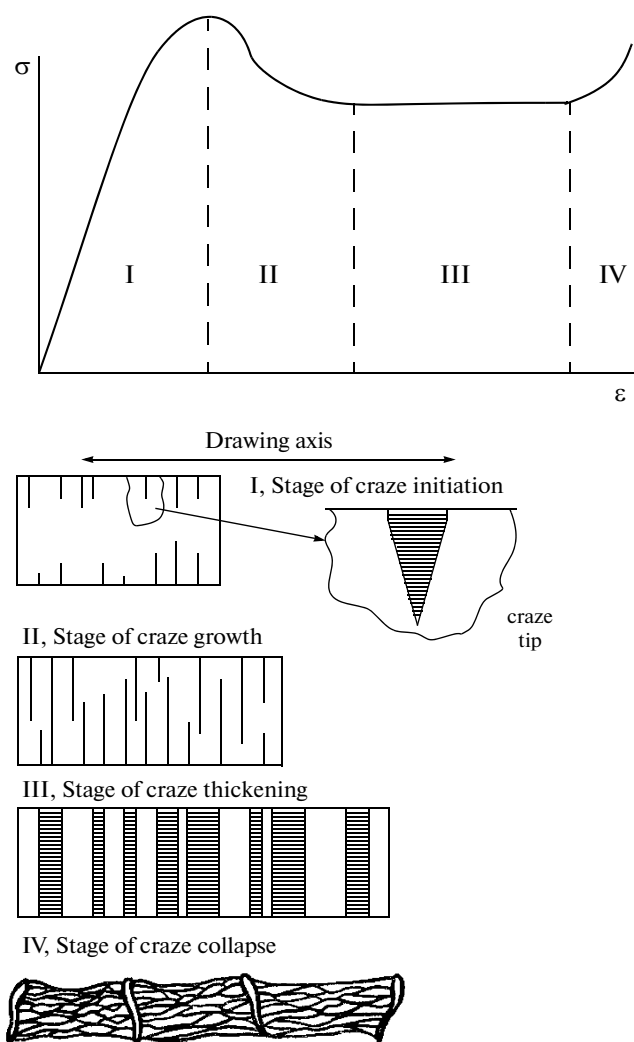


**Fig. 1.** Stress-strain curves of the polymer in AAM and schematic representation of the individual stages of the development of crazes: I, region of the initiation of crazes; II, region of the growth of crazes; and III, region of the thickening of crazes.

## 2. SOLVENT CRAZING AS A METHOD FOR PREPARING POLYMERS WITH NANOSCALE POROSITY

The crazing of polymers in liquid media represents one of the fundamental types of inelastic deformation of solid polymers [23, 24]. This kind of deformation, which is actually a manifestation of the Rehbinder effect in polymers [25, 26], leads to dispersion of the solid polymer into small aggregates of oriented macromolecules (fibrils) separated by microvoids of approximately the same size. The deformation of a polymer by the mechanism of solvent crazing can be easily implemented when the polymer is drawn in so-called adsorption-active media (AAM) [21, 22] and occurs through the formation and development of special zones of plastically deformed polymer: crazes.

The process of deformation during crazing can be divided into several stages, and the contribution of each to the formation of the porous structure in the polymer can be assessed [21, 22]. The stress-strain curve and the general evolution of the structure depending on the tensile strain of the polymer in the AAM are shown in Fig. 1. The first stage is the formation of crazes. It has been established that this process is locally critical and associated with loss of the stability of the defects of the real polymer. Here, the role of the defect can be performed by uneven surface topography, variations in polymer structure, and various mechanical impurities. The number of nucleated crazes can be adjusted by changing the defectiveness of the initial polymer, by conducting preliminary formation of a large number of crazes under more severe conditions of deformation [27], or by using preorientation of the polymer [28]. The stage of appearance

of crazes is important for the formation of the porous structure in the deformed polymer, because at this stage one can adjust the density of crazes, which depends on the deformation conditions and defines such technological characteristics as the uniformity of pore distribution in porous materials.

The second stage is the growth of crazes in the direction perpendicular to the drawing axis. This stage lasts until the individual crazes or their ensemble grows through the entire cross-section of the sample. For the development of crazes, the drawing should be done under such conditions that the medium has enough time to penetrate the local deformation zone at the top of the craze. It follows that the critical parameters of the development of crazes and formation of the porous structure in the deformed polymer are the strain rate, the scale factor of the samples (particularly, their thickness), and the coefficient of hydrodynamic resistance of the resulting fibrillar–porous structure of the craze to the liquid flow [29, 30]. The last parameter, in turn, is determined by the diameter of pores in the crazes and the viscosity of the medium in which the drawing occurs.

The third stage of the development of crazes is their thickening in the direction parallel to the drawing axis. This stage is the most important in terms of obtaining materials with high porosity. The main parameters affecting the rate of the thickening of crazes as a function of deformation conditions remain the same as those for the linear rate of the growth of crazes [31]. In the consideration of this phase, the main attention is focused on the mechanism of the drawing of fibrils in crazes. Depending on the nature of the medium (AAM or a medium providing the plasticizing effect on the polymer), either the mechanism of the surface drawing of fibrils or the mechanism of creep can be implemented.

However, there is one more step that is observed at even higher tensile strain, that is, the collapse of the fibrillar–porous structure of crazes. At this stage, a narrowing of the sample occurs, while the fibrils in crazes undergo orientation drawing. In essence, this stage limits by the tensile strain of the area in the deformed polymer where the porous structure can be formed. However, this stage of the development of crazes is important for sealing their porous structure and for obtaining monolithic materials. The evolution of the porous structure during polymer crazing is described more thoroughly in [32]. This kind of deformation of a polymer in adsorption-active media was given the name “classical localized crazing.”

In addition to the classical crazing described above, for which the stages of development of individual crazes can be clearly observed, there is another kind of deformation of polymers in liquid media: delocalized crazing [33, 34]. If classical localized crazing is more typical for amorphous glassy polymers, the delocalized crazing is characteristic only for crystalline polymers. As a result of the development of deformation by the mechanism of delocalized crazing, a nanoporous structure also appears in the polymer, but in a different way. In this case, the development of porosity occurs simultaneously throughout the entire volume of the polymer, and the polymer is a homogeneous nanoporous material at all stages of deformation. The structure of the polymers deformed by the mechanism of delocalized crazing can also be represented by fibrils oriented along the drawing axis of the polymer and the voids between them.

A common feature of the structures of crazed polymers formed by drawing via the mechanisms of both classical and delocalized crazing is that the fibrils and the microvoids between them have nanoscale dimensions and are approximately 2–20 nm. The total porosity in this case can reach 60%, while the specific surface area of fibrillar polymer can be more than 100 m<sup>2</sup>/g. The size of pores and fibrils in the crazes can be controlled by adjusting the tensile strain of the polymer, the nature of the AAM, the temperature–power modes of the drawing, the degree of preliminary orientation, and the structure of the original polymer.

There is another structural feature of a crazed polymer. During the deformation of the polymer in the AAM by the mechanism of crazing or by drawing in air, the orientation of the polymer takes place. However, the orientation of macromolecules occurs not in a monolithic neck but in the finest fibrillar aggregates of macromolecules separated in space. The oriented structure of these materials ensures their excellent mechanical properties, despite the presence of through porosity. However, it creates certain difficulties in obtaining stable nanoporous materials, related to the prevention of further shrinkage of the deformed samples.

Thus, the crazing of polymers in adsorption-active media can be implemented for a wide range of amorphous, glassy, and crystalline polymers and is accompanied by the formation of a highly dispersed fibrillar–porous structure.

### 3. PECULIARITIES OF THE FORMATION OF POLYMER–POLYMER BLENDS BASED ON POLYMERS DEFORMED IN LIQUID MEDIA BY THE MECHANISM OF SOLVENT CRAZING

#### 3.1. Peculiarities of the Formation of Polymer–Polymer Blends by In Situ Polymerization in a Solvent-Crazed Polymer Matrix

A unique fibrillar–porous structure can only appear during the crazing if the formed pores are continuously filled with the ambient liquid medium in which the polymer is deformed. If the drawing is carried out in a solution containing some additives, the additives penetrate the nanoporous structure of crazes with the solvent. As a result, both the polymer and the low-molecular substance thermodynamically incompatible with the polymer are not only mutually dispersed at the nanoscale level but also, which is important, form a highly dispersed and rather homogeneous blend.

Naturally, such features of the crazing of polymers in liquid media create preconditions for the development of a universal method for introducing a second component into polymers in order to obtain a nanocomposite material. The possibilities of crazing as a method for creating nanocomposites with low-molecular substances of different nature have been rather widely discussed [35]. In this paper, we will consider issues associated with various methods of obtaining blends on the basis of crazed polymers and with the characteristics of their structure and some physicomechanical properties.

One of the methods for generating blends is based on the polymerization of monomers performed in a matrix of crazed polymer (in situ polymerization). We will give some examples of blends obtained using this method, based on polymers deformed by the mechanism of classical crazing. Nanopores in the crazes are open and interconnected and can be filled with the monomer both in tension and by the subsequent change of the medium used for drawing the monomer. For example, composite materials were obtained based on crystalline polyethylene terephthalate (PET) deformed by the mechanism of classical crazing and polyvinylpyrrolidone (PVP) [36]. At the same time, the drawing of PET to different degrees was carried out directly in vinylpyrrolidone, and the subsequent polymerization of the monomer was performed using  $\gamma$ -irradiation.

Electrically conductive blends based on amorphous PET, also deformed by the mechanism of conventional crazing, and polyaniline were obtained in [37–39]. In this case, PET was predrawn to various tensile strain in an adsorption-active medium (*n*-butanol). Then, the medium was replaced with the monomer solution, and the polymerization of aniline was carried out electrochemically under galvanostatic conditions.

The results showed that the use of porous substrates obtained using classical crazing yields blends with a high concentration of the introduced polymer. In this case, the distribution of the introduced polymer in the blend is determined by the specific structure of the crazed polymer. Depending on the tensile strain, as shown in the diagram presented in Fig. 1, the resulting material can be composed of alternating sections of the initial undeformed polymer and the blend consisting of fibrillar PET and the second polymer that fills the porous structure of the crazes. Only with large deformations exceeding the natural draw ratio of PET (300%), when there are no sections of the undeformed polymer, does the structure of the blend become homogeneous. The concentration of the introduced polymer in the blend varies according to the change in the porosity of the deformed PET and, as shown in Fig. 2, reaches a maximum of 150–200%.

In contrast to classical crazing, delocalized crazing is carried out uniformly over the entire sample volume, which makes it more attractive for obtaining new types of polymer–polymer blends. As noted above, the delocalized crazing is performed only during the deformation of crystalline polymers. At the same time, virtually all IPNs known today are synthesized on the basis of amorphous polymers. This is due to the fact that the preparation of polymeric nanocomposites by in situ polymerization involves the ability of the so-called first polymer network to swell considerably in the second monomer [40, 41]. Crystalline polymers such as polyethylene (PE) or polypropylene (PP) are capable of only limited swelling in organic liquids having an affinity for them. Swelling of this kind is usually small and only a few percent, because the low-molecular-weight component is able to penetrate only into the amorphous regions of the polymer and does not affect the crystallites. Therefore, it is natural that a highly crystalline polymer such as high-density polyethylene (HDPE) is unable to absorb significant amounts of a low-molecular-weight liquid, in particular, a monomer. It is probably for this reason that IPNs based on crystalline polymers have not been synthesized.

The crazing of polymers in liquid media can dramatically increase the amount of a low-molecular-weight component in the deformed polymer. As was shown in [42], the stretching of the polymer in contact with the plasticizing liquid can increase its swelling to 100% or more. This fact was used in [43] to obtain a number of polymer blends based on HDPE. In this paper, monomers that cause the delocalized

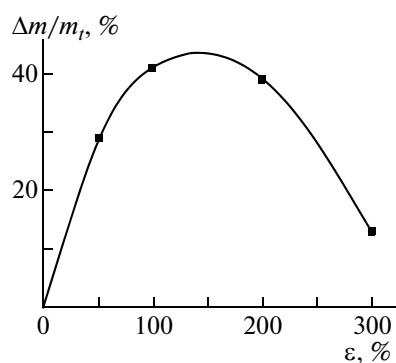


Fig. 2. Dependence of the concentration of polyaniline in the blend of PET–polyaniline on the tensile strain of PET.

crazing of a polymer and actively penetrate into the developing porous structure of crazes were used as an active liquid.

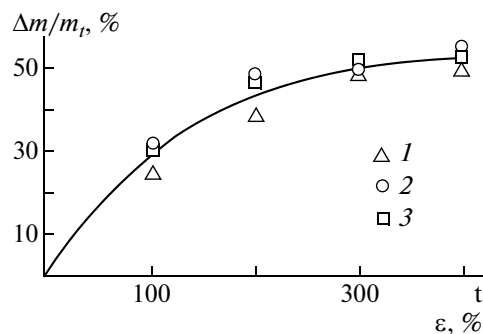
In order to obtain polymer compositions, a film of extruded HDPE was stretched at room temperature in monomers containing 0.3 wt % of an initiator (benzoyl peroxide) and, in some cases, a cross-linking agent. Monomers that are compatible with HDPE were selected: methyl methacrylate (MMA), styrene, and *n*-butyl methacrylate. After the deformation to the desired tensile strain, the sample size was fixed in a special frame; then, the sample was transferred to a thermostatically controlled vessel where polymerization was carried out. As can be seen, the methodical creation of the polymer–polymer nanocomposite in this case is completely analogous to the method for producing serial IPNs [2].

Figure 3 shows the amounts of the polymer introduced by polymerizing the corresponding monomer as a function of the tensile strain of HDPE in the liquid monomer. It is clearly seen that the method described above can produce HDPE-based nanocomposites containing up to 50% or more of the second component, which, naturally, would be impossible to achieve with a simple swelling of the undeformed polymer in the same monomers. The amount of the second polymer increases monotonically with increasing degree of polymer stretching and comes close to the limit with the elongation of approximately 200–250%, in exactly the same way as the amount of the plasticizing liquid in which the deformation is carried out [42]. The amount of the second component introduced into HDPE does not depend much on the nature of the selected monomers, and the dependence on the degree of predrawing of HDPE in all selected monomers can be approximately described by a single curve.

Since both components of the blend were linear in the cases where the cross-linking agent was not added, it was possible to verify the data obtained by the selective washing of components. This approach is often used for analyzing the composition and structure of polymer compositions, in particular, interpenetrating polymer networks [44, 45]. For this purpose, the compositions based on HDPE–polymethylmethacrylate (PMMA) were successively washed in chloroform (for the dissolution of PMMA) and *n*-decane (for dissolving HDPE). Independent experiments showed that the homopolymers were completely dissolved under the same conditions. The results of these experiments are presented in Fig 4. It turns out that the components of the resulting composition are not completely separated by selective dissolution. In all cases, approximately 25–30 wt % of insoluble products remain after washing. Apparently, either chemical grafting of the chain of components [41] or their interpenetration at the molecular level (as observed in a majority of interpenetrating polymer networks [46]), or the simultaneous occurrence of these processes, takes place under polymerization conditions.

Nevertheless, the resulting blends are biphasic systems. Figure 5a shows an electron microphotograph of a PMMA-frame obtained after HDPE is washed from the blend. It is clearly seen that the removal of HDPE leads to the formation of a high-openwork frame with the structural element dimensions ranging from a few nanometers to a few tenths of a micron. A similar pattern is observed in the case when PMMA is washed from the blend (Fig. 5b). Obviously, the structures shown in Figs. 5a and 5b are complementary, and they reinforce each other. The biphasic properties of the resulting blends were also confirmed by calorimetry; according to the data obtained, there is no change of temperature and heat of fusion of HDPE [43]. Thus, the proposed procedure allows the achievement of the goal, namely, the creation of a new type of polymer–polymer nanocomposites.

It is important to emphasize that the HDPE-based polymer blends produced by in situ polymerization markedly differ morphologically from similar compositions obtained in the conventional way (by mixing



**Fig. 3.** Dependence of the concentration of (1) PMMA, (2) PS, and (3) PBMA in the composition on the tensile strain ( $\epsilon$ ) of HDPE in the corresponding monomer.

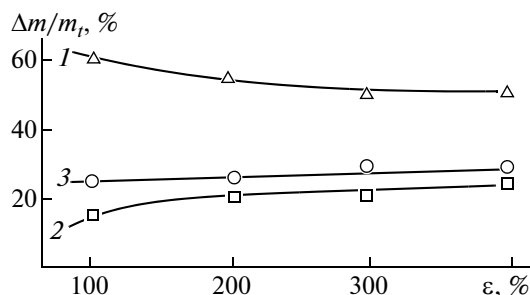


**Fig. 4.** Dependence of the concentration of (1) HDPE, (2) PMMA, and (3) the residue of HDPE insoluble in selective solvents in the composition of HDPE-PMMA on the tensile strain ( $\epsilon$ ) of HDPE in methylmethacrylate.

polymer melts), regardless of whether graft or block copolymer, if any, is added to this blend to improve the compatibility. For example, in the blends based on the PE-PS blends of any composition, spherical structures appear with dimensions of 1–10 microns in the continuous matrix [47–49]. This morphology occurs in the melt under the action of surface forces due to the incompatibility of components. It is obvious by the sizes of the coexisting phases that such a blend cannot be termed nanocomposite.

For the blends obtained by crazing, spherical formations of one component are not observed, and, as seen in Fig. 5, a significantly higher level of dispersion is achieved for the coexisting phases, whose dimensions are characteristic for nanocomposites. This is explained by the fact that the formation of the second polymer phase occurs in intercrystallite and interfibrillar regions of HDPE. Under conditions of the polymerization of the second monomer (styrene), HDPE is lower than its melting temperature and is capable of resisting the effect of surface forces determining the phase separation, thereby stabilizing the resulting structure. In other words, the network of HDPE crystallites limits the possibility of formation of the elongated phase of the second component and determines the dispersion of the system. The situation is similar to the case observed in the synthesis of interpenetrating polymer networks, when the increase in cross-link density of the first network increases the phase dispersion of the emerging second network [50]. In this case, the crystal structure of HDPE plays the role of cross-links in the first network.

On the basis on these data, one can conclude that, in the synthesis of the described polymer blends, a structure having a dual phase continuity is formed, because the selective washing of each component leads to the formation of a continuous porous skeleton rather than to the disintegration of the sample into pieces.

It should be noted that the increase in the tensile strain of HDPE in a liquid monomer leads not only to an increase in the amount of the second component in the blend. According to data presented in [43, 51], a noticeable orientation of HDPE occurs in the process of stretching. At the same time, the introduction of the second polymer component into HDPE is not accompanied by its molecular orientation. It is obvious that the change in the molecular orientation of one of the components during crazing should affect the properties of the final product. In other words, unlike the known approaches for obtaining poly-

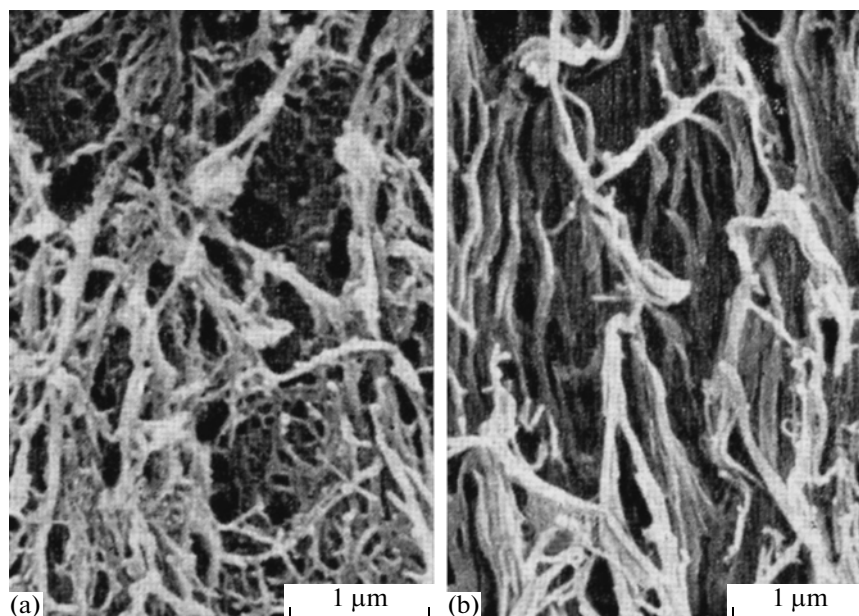


**Fig. 5.** Electron micrographs of nanocomposite HDPE–PMMA (tensile strain in the monomer, 200%) after the selective washing of (a) HDPE and (b) PMMA.

mer–polymer blends, the crazing of polymers uses another factor having a directional effect on the properties of the resulting nanocomposites.

Thus, the radical polymerization of several monomers in a matrix of HDPE deformed in their environment provides a number of interesting polymer–polymer blends having a high mutual dispersion of components. Using the stretching of the polymer in a liquid monomer, a wide range of crystalline polymers can be included in the number of objects suitable for creating blends by in situ polymerization, such as HDPE [43, 51, 52], polypropylene (PP) [53–55], and polyamide (PA-12) [56], blends of which are usually prepared only by mixing their melts. Naturally, high degrees of dispersion of components were impossible to reach in these cases, which had an undesirable effect on the properties of the resulting materials. Moreover, nanocomposites based on polymers that differ significantly in polarity, for example, polytetrafluoroethylene and polyacrylamide [57] or polypropylene and polyacrylamide [58], can be created using crazing. The combination of these polymers in one material by conventional methods obviously represents significant difficulties.

### *3.2. Direct Introduction of the Second Polymer Component into the Polymer Deformed by the Mechanism of Solvent Crazing*

In the above cases, in order to obtain the polymer–polymer nanocomposite, a monomer is introduced into the porous structure of the crazed polymer, and the monomer is then polymerized in situ. This approach was dictated by the fact that the direct introduction of macromolecules into nanopores of the crazed polymer was believed to be difficult for steric reasons. Indeed, even for one of the most flexible chain polymers—polyethylene—the unperturbed dimensions of a macromolecule with a molecular mass of 1 million are of the order of 200 nm. At the same time, the size of the nanopores in the structure of crazes varies from 2 to 20 nm. However, it is obvious that, if we could include a macromolecule in any manner in the structure of the crazed polymer, it would greatly simplify the procedure for obtaining polymer–polymer blends, because this would exclude the very time-consuming and environmentally unsafe stage of polymerization from the process of producing polymer–polymer blends.

In this regard, recent studies were carried out to ascertain if macromolecules can be directly introduced into the nanoporous structure of crazed polymers. The creation of blends based on polymers having dramatically different properties, e.g., hydrophilic and hydrophobic, seems to be the most promising to clarify this possibility. In this case, we can assume the appearance of the most interesting and unexpected properties of the resulting polymer product. The combining of these components, which are very different in polarity, is a serious problem itself. For example, nonpolar polymer PET and polar polymers polyethylene glycol (PEG) and polypropylene glycol (PPG) cannot be combined with the formation of a highly



dispersed blend by any known method. Indeed, the melting temperature of PET is 252°C, and the temperature of chemical decomposition of PEG and PPG is 180 and 220°C, respectively. It is obvious that these components cannot be mixed with each other through the mixing of their melts. The mixing of such different polymers in solution is also difficult to implement, since these polymers do not have common solvents. Thus, the use of crazing is probably the only realistic means for obtaining nanocomposites based on these components.

To create polymer blends by direct tensile drawing in solutions of macromolecular compounds, a wide range of polymers with a molecular weight of 400 to 1 million or more were used. It was found that liquid oligomers such as PEG and PPG are themselves effective crazing agents for PET and HDPE [59]; therefore, they are included in the porous structure of the polymer deformed in their environment, resulting in a polymer–oligomer nanocomposite. The quantity of the included second component is rather high (up to 40 wt % or more); therefore, we can expect that it has a significant effect on the properties of the final product.

However, there are some limitations in obtaining oligomer–polymer blends at high rates of deformation. Liquids in which the polymer practically does not swell but which reduce its surface tension are usually used as AAM for crazing. However, along with a decrease in the surface energy of the polymer, another demand is made of AAM, associated with the kinetics of the transport of liquid to the top of the growing craze. For the effective development of crazing, the environment should manage to enter the tip of the growing craze. Otherwise, the deformation of the polymer is carried out in air with the development of the neck [29]. One of the parameters that determines the flow velocity of the liquid is its viscosity, and the transition from crazing to shear is most notably manifested in the deformation of polymers in highly viscous environments, in particular, PEG and PPG. The issues related to the kinetic difficulties of the transportation of highly viscous liquid oligomers to the tip of developing crazes were more thoroughly considered in [60, 61].

In this connection, the question arises of whether polymers with higher molecular weight (in particular, the solids PEG or PEO with molecular weight up to 1 million) can be introduced into the nanoporous structure of the crazes. It is obvious that, to introduce solid polymers, it is necessary to use their solutions in AAM, because crazing can be realized only in the presence of liquids or gases. In [60–63], the deformation of PET and HDPE was carried out in solutions of PEO in ethanol–water mixtures. The solvent composition was selected so that, on the one hand, it dissolved a significant amount of PEO, and on the other hand, the same solvent caused an effective crazing of matrix polymers. The concentration of polymers in the solution was 5–20 wt %.

Surprisingly, such polymers with high molecular weight (up to 1 million) are able to effectively penetrate into the nanoporous structure of crazed PET, forming the corresponding polymer blends with a high content of the second component (Fig. 6, curve 1). Note that the penetration of PEO into the porous structure of PET is carried out under conditions where the coil diameter of macromolecules in solution greatly exceeds the size of the pores of the polymer deformed by the crazing mechanism. The effective pore diameter of PET under drawing in AAM, determined by the method of liquid permeation under a pressure gradient or by small-angle X-ray scattering, is 5–10 nm, while the mean square radius of the coil of PEO macromolecules with molecular weight from 40 000 to 1.2 million is 9.2–63 nm [61–63]. In addition, one may assume that the high viscosity of polymer solutions used for drawing, which is significantly higher than the viscosity of liquid oligomers, will also hinder the development of polymer deformation by the crazing mechanism, and it would be impossible to obtain the blends by the method of direct drawing.

However, it was found that the deformation of polymers in solutions of macromolecular compounds is carried out by the crazing mechanism and that macromolecules penetrate into the nanoporous structure of the crazes. Moreover (Fig. 6), the amount of PEO penetrating in the process of crazing in both the PET deformed by the mechanism of classical crazing and in the HDPE deformed by the mechanism of delocalized crazing far exceeds its potential concentration, which can be calculated on the assumption that the porous structure is completely filled with the surrounding polymer solution (Fig. 6, curve 2). In other words, there is some mechanism for the enrichment of PEO solution that penetrates into the porous structure of PET and HDPE, which develops in the process of their crazing in the deformation of the second polymer component in the solution. It was suggested that the high concentration of PEO in the blends was due to its adsorption on the highly developed surface of the fibrillized polymer in the crazes [62].

Many features of this process have yet to be fully clarified. However, it can be assumed that the creation of polymer blends by the direct introduction of a second polymer component during the drawing process is quite achievable.

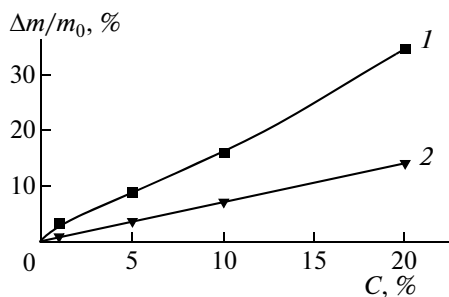


**Fig. 6.** Dependence of the content of PEO with molecular weight 40000 in the blend PET-PEO on (1) the concentration of PEO in the solution and (2) theoretical curve.

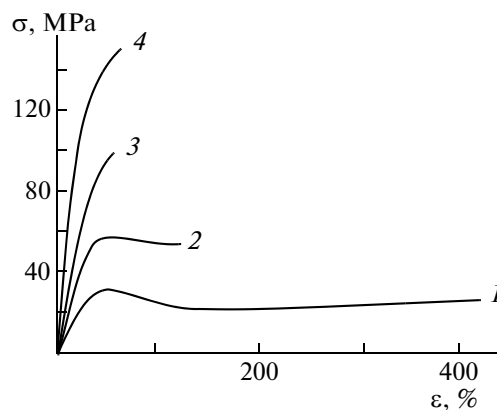


**Fig. 7.** Stress-strain curves of HDPE preoriented in *n*-heptane by (1) 100, (2) 200, (3) 300, and (4) 400%.

#### 4. PHYSICOMECHANICAL PROPERTIES OF POLYMER BLENDS OBTAINED BY SOLVENT CRAZING

##### 4.1. Mechanical Properties of Polymer Blends Obtained by *In Situ* Polymerization in a Solvent-Crazed Polymer Matrix

The stress-strain curves for HDPE subjected to drawing in *n*-heptane to tensile strains by the mechanism of delocalized crazing are presented in Fig. 7. It is clearly seen that the polymer matrix used for obtaining new types of nanocomposites shows a behavior characteristic of oriented polymers. During drawing, the modulus, yield strength, and durability of the polymer increase and its elongation decreases [52].

Let us now consider how the mechanical properties of polymer blends change, if one conducts the *in situ* polymerization of the second polymer in crazed PE according to the procedure described in the previous section. Figure 8 shows the stress-strain curves of the blends of HDPE with PS or PMMA. It is clearly seen that the resulting blends “remember” that the phase of PE is oriented. Indeed, with increasing degree of preliminary elongation of HDPE in a particular monomer, the modulus and yield strength of the obtained material increases regularly. As seen in Figs. 8a and 8b, the second component, which is in the glassy state, also has a significant influence on the properties of the composite, which is primarily reflected in an increase of the initial modulus of the obtained material. At the same time, in all cases, the polymer blend acquires properties that are not characteristic for any of its components. It is seen that nanocomposites based on HDPE and PS, as well as on HDPE and PMMA, are capable of large plastic deformations. Indeed, the introduction of PS or PMMA into HDPE enables the achievement of significant elongation, even for the blends based on HDPE deformed by 300–400% and incapable of noticeable lengthening in its pure form (Fig. 7). As we know, neither PS nor PMMA is capable by itself of significant inelastic deformations at room temperature, and they disintegrate at an elongation of 3–5%. Moreover, even cross-linking of the glassy component in the blend structure (Fig. 8) does not inhibit its capacity for large plastic deformations. Thus, there is a synergism in the mechanical behavior when the two polymers,

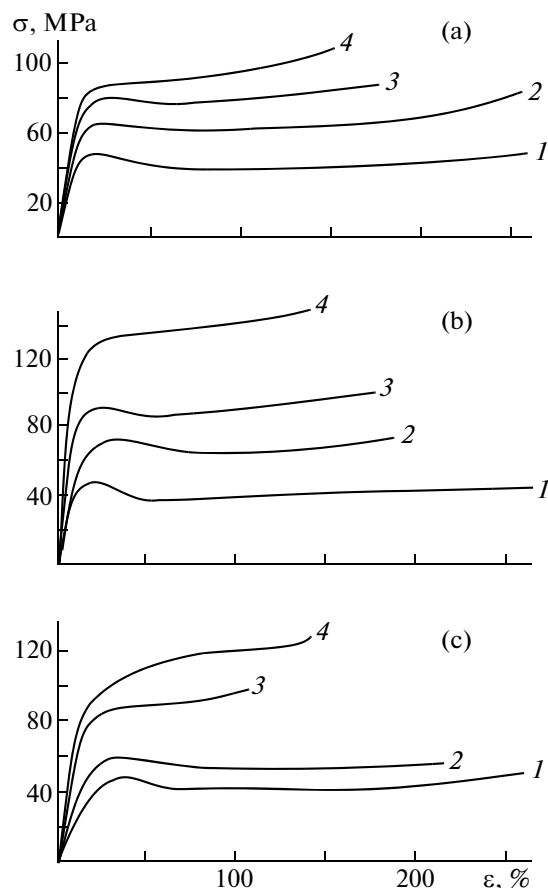


**Fig. 8.** Stress-strain curves of composites based on (a) HDPE–PS and (b and c) HDPE–PMMA, obtained by in situ polymerization using the drawing of HDPE in (a) styrene or (b and c) methylmethacrylate by (1) 100, (2) 200, (3) 300, and (4) 400% (b) without cross-linking agent or (c) in the presence of 20 wt % of ethylene glycol dimethacrylate.

which are individually incapable of significant deformations, exhibit such an ability, being connected to the nanocomposite structure.

Apparently, the reasons for the observed synergy lie in the high dispersion of the glassy polymer injected into the PE matrix. The studies of the last decade show that, in thin layers (nanoscale thickness range) of glassy polymers, a sharp decrease in their glass transition temperatures (by tens and hundreds of degrees) occurs [64, 65]. The data of various authors on the measurement of the glass transition point ( $T_g$ ) of PS, depending on the thickness of the polymer film [66], are shown in Fig. 9. It is clearly seen that there is a strong decrease in  $T_g$  beginning with film thicknesses of a few hundred angstroms. The reasons for this strong decrease in the glass transition point of polymers entering the nanostate are detailed in [64–66].

In other words, the transition of the polymer to the nanostate is accompanied by a significant change in its properties and, in particular, by a sharp decrease in  $T_g$ . The decrease of  $T_g$  below the test temperature (room temperature) means that the amorphous polymer in the matrix of HDPE is in the rubbery state and therefore loses its brittleness. The matrix material is transformed to the nanostate as well and, apparently, also changes its properties. As a consequence, the resulting nanocomposite has a greater flexibility than its constituent block polymers.

It is important to note that the system keeps its valuable mechanical properties as long as the polymer blend is dispersed to the nanostate.

The annealing of the obtained materials above the melting point of the crazed polymer matrix leads to irreversible changes in the structure of the obtained polymer blends. Structural studies show that a significant increase in the phase domain of components occurs [67]. As a consequence, the received films lose their strength and ductility to a great degree and are destroyed at low values of tensile strength (~5 MPa) and elongation (2–5%). In fact, in this case, the resulting polymer blend ceases to be a nanocomposite, and a structure appears that is usually implemented with a mixture of polymers from the melt [49].

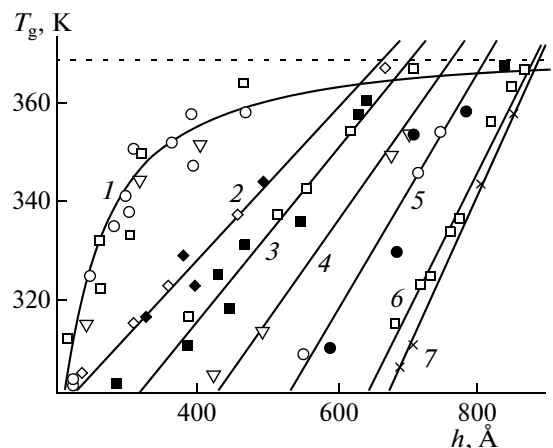


**Fig. 9.** Dependence of the glass transition point of free PS films (with different molecular weight of PS,  $M \times 10^{-3}$  g/mol) on their thickness  $\text{\AA}$ : (1) 116–347, (2) 541, (3) 691, (4) 1250, (5) 2077, (6) 6700, and (7) 9000 [33]. The dotted line shows the glass transition temperature of block PS.

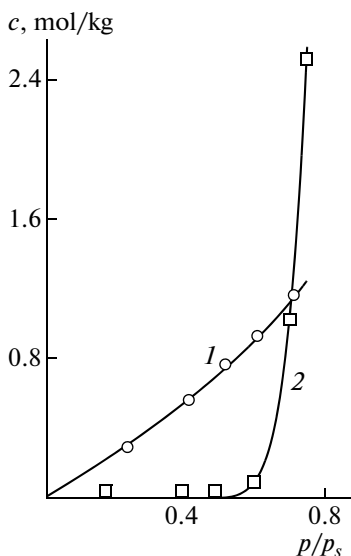


**Fig. 10.** Isotherms of adsorption of  $\text{CCl}_4$  into (1) the IPP sample deformed in *n*-heptane by 200% and (2) the IPP–PMMA composite obtained in the deformation of IPP in MMA by 200%.

For example, the elongation of the blends of PE and PS, obtained by mixing of their melts and containing 50% of each component (i.e., similar in composition to that discussed above), ranged from 2 to 8%, and their tensile strength was less than 10 MPa.

Thus, the introduction of an amorphous component into HDPE by in situ polymerization results in nanocomposites with enhanced strength and ductility.

#### 4.2. Adsorption Properties of Polymer–Polymer Nanocomposites Obtained by in situ Polymerization in a Solvent-Crazed Polymer Matrix

Investigation of the diffusion and adsorption of low-molecular compounds into polymers provides important information not only about the mechanism of transport but also about the structure of the material. While the transport processes in single-component polymers are rather well studied [68], studies of this kind regarding multicomponent heterophase polymer blends are still few in number and have not yet found broad generalization. Only a few works are devoted to the adsorption properties of nanocomposites obtained using crazing [69, 70], which certainly cannot fully cover their properties.

Let us consider some results of a study of diffusion and adsorption of a selective low-molecular solvent into the structure of a nanocomposite based on isotactic polypropylene (IPP) and PMMA, obtained by

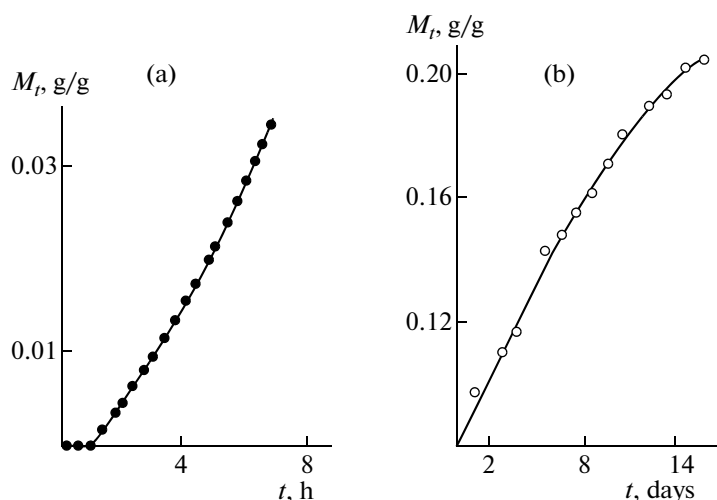


**Fig. 11.** Kinetic curves of the adsorption of  $\text{CCl}_4$  into the IPP-PMMA composite obtained in the drawing of IPP in MMA by 200%: (a) initial section and (b) stationary section;  $p/p_s = 0.69$ .

the above method [69]. Typical adsorption isotherms of  $\text{CCl}_4$  in IPP, deformed in *n*-heptane by 200%, and in a mixture of IPP in PMMA, obtained by the drawing of PPI in methylmethacrylate by 200%, followed by its in situ polymerization are shown in Fig. 10. It is clearly seen that pure IPP has a usual adsorption isotherm, characteristic of a crystalline polymer that is above the glass transition temperature [71]. This isotherm is almost identical to the adsorption isotherm of the initial nonoriented IPP. At the same time, the adsorption isotherm of  $\text{CCl}_4$  in the composite has a number of features that are not characteristic of a crystalline polymer.

First, up to significant values of the vapor pressure of  $\text{CCl}_4$  ( $p/p_s \sim 0.5-0.6$ ), the adsorption of  $\text{CCl}_4$  in the composite does not occur. After the vapor pressure reaches a certain threshold value, the adsorption begins to rise very sharply. This curve resembles the isotherm of water adsorption by low-molecular-weight sugar, which is due to its melting and subsequent absorption of water by the resulting solution [72]. Since the water and sugar are mixed in all ratios, there is a sharp rise in a narrow range of vapor pressure in the adsorption isotherm of this system. In the considered case, such physical phenomena obviously do not take place. Nevertheless, as seen from Fig. 10, the quantity of  $\text{CCl}_4$  adsorbed by the polymer blend increases dramatically and noticeably exceeds the amount absorbed by pure IPP. Secondly, with vapor pressures greater than 0.6 the equilibrium value of adsorption cannot be reached, because the process continues for many days. To analyze such unusual adsorption behavior of a blend of IPP with PMMA, we consider the data on the kinetics of adsorption. In the case of the initial nonoriented IPP and IPP extended in an active liquid, the adsorption curve has the usual form, which reaches an equilibrium value in approximately 1 h. The introduction of PMMA into the IPP matrix dramatically changes the kinetics of the adsorption process. As can be seen from the data presented in Figs. 11a and 11b, the adsorption develops linearly after a short induction period. This character of adsorption persists for many days (Fig. 11b) or even weeks. The equilibrium value of adsorption is not achieved even in 1 month. The adsorbed amount of  $\text{CCl}_4$  reaches 50 or more wt %, although the pure initial IPP, which is the only component that has an affinity to  $\text{CCl}_4$ , absorbs no more than 15%.

The behavior of the blends in the desorption of  $\text{CCl}_4$  is also unusual. When the vapor pressure decreases, the samples of pure IPP exhibit a reversible change in adsorption, and under vacuum they completely lose all adsorbed  $\text{CCl}_4$ . At the same time, in the case of a blend of IPP with PMMA, the exposure of the samples that adsorbed at the vapor pressure of adsorbate of 0.7 from the saturated vapor pressure at a pressure of 0.6 for 2 days does not lead to the loss of the adsorbate, which can be detected using a quartz balance. Nor does the exposure of the same sample in air for 20 days at room temperature cause a noticeable desorption of  $\text{CCl}_4$ . Only the combined effect of vacuum and increasing temperature from room temperature ( $23^\circ\text{C}$ ) to  $40^\circ\text{C}$  can cause a partial desorption of  $\text{CCl}_4$ .

Thus, the introduction of glassy PMMA in IPP by polymerization in a polymer matrix drastically changes the adsorption characteristics of IPP. A number of questions arise. What explains the unusual form of adsorption isotherms, and why is there a threshold of the vapor pressure of  $\text{CCl}_4$ , below which the adsorption is not observed? What explains the unusual kinetics of adsorption and the ability of the com-

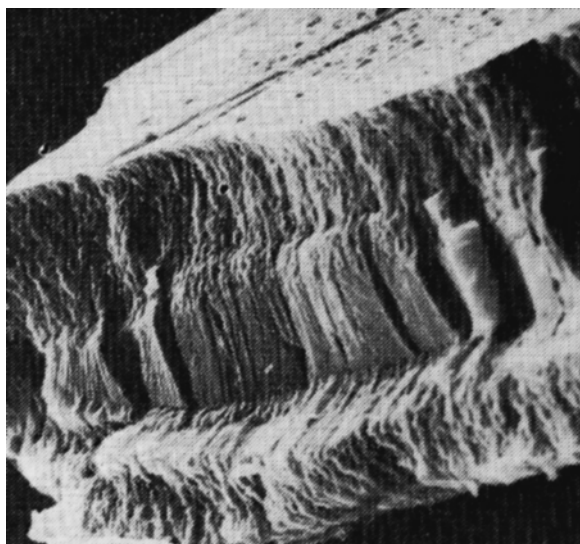


**Fig. 12.** Scanning electron micrograph of a brittle cleavage of the IPP–PMMA nanocomposite after the adsorption of  $\text{CCl}_4$  from the liquid phase for 30 days.

posite to absorb such large amounts of  $\text{CCl}_4$ , although pure IPP is capable of absorbing several times smaller amounts of  $\text{CCl}_4$ , while pure PMMA does not absorb it at all? Why is the desorption of  $\text{CCl}_4$  from the blend largely irreversible or very difficult?

It was found that this unusual behavior of the resulting blends was due to structural rearrangements occurring in the material upon the penetration of the low-molecular-weight component [69]. It turned out that on both surfaces of the sample, that is, where the film had interacted with  $\text{CCl}_4$ , its structure was looser than the dense core (Fig. 12). There was a very sharp boundary between the loose shell and the dense core. It is the emergence of a loose porous structure that causes such large amounts of absorbed  $\text{CCl}_4$  by its condensation occurring in formed microvoids.

The performed calculations together with given electron microscopic data suggest the following mechanism for this phenomenon. The creation of small vapor pressures does not cause a noticeable swelling of the composite due to the fact that IPP, which is capable of swelling in  $\text{CCl}_4$ , is in a rigid frame of PMMA impeding the change in the size of the IPP phase. This continues until the condensation of  $\text{CCl}_4$  starts in the narrow surface pores characteristic of the composite structure. The emergence of the liquid  $\text{CCl}_4$  films of such small sizes leads to disjoining pressure, which plays an important role in the stabilization of dispersed systems [73]. As a result of the disjoining pressure, a kind of spontaneous dispersion of the nanocomposite structure, which is built of thermodynamically incompatible polymer components, occurs. This kind of spontaneous dispersion occurring by the penetration of liquid along the boundaries between the grains is well known and described in detail for low-molecular dispersed systems [74].

Thus, the introduction of a glassy component in IPP using polymerization in a polymer matrix drastically changes the nature of the adsorption of a selective low-molecular-weight solvent. A kind of synergy in adsorption is observed, when the adsorption value increases sharply with the introduction of the second component that does not interact with the adsorbate. The unusual adsorption behavior of polymer blends is due to its peculiar spontaneous dispersion, which leads to a decay into separate phases and to a number of phenomena that are not characteristic for any of the pure components.

#### *4.3. Electrically Conductive Polymer Blends Obtained by in situ Polymerization in a Solvent-Crazed Polymer Matrix*

In the context of this review, it seems important to highlight also the data on the creation of blends in which one of the components is an electrically conductive polymer. The preparation of new types of conductive polymers is among the most important scientific and applied problems of the modern physical chemistry of polymers. Despite the considerable progress achieved in recent years in this field, the practical use of conductive polymers is rather limited, because as a rule they are nonfusible, insoluble powders that are barely suitable for recycling [75].

**Table 1.** Composition and conductivity of the blends with conductive polymers;  $\lambda$ , tensile strain of the polymer;  $C$ , content of the conductive polymer in the blend;  $\sigma_v$ , specific volumetric electrical conductivity;  $\sigma_s$ , specific surface conductivity in two directions;  $A$  is anisotropy of the specific bulk electrical conductivity

Blend	$\lambda$ , %	$C$ , %	$\sigma_v$ , $\Omega^{-1} \text{ cm}^{-1}$	$\sigma_s$ , $\Omega^{-1} \text{ cm}^{-1}$		$A$	
				$\sigma_s^\perp$ , $\Omega^{-1} \text{ cm}^{-1}$	$\sigma_s^\parallel$ , $\Omega^{-1} \text{ cm}^{-1}$	$\sigma_s^\perp / \sigma_s^\parallel$	$\sigma_s^\parallel / \sigma_s^\perp$
PET–polyaniline	50	29	$1.6 \times 10^{-3}$	$3.7 \times 10^{-2}$	$5.4 \times 10^{-3}$	6.8	—
	100	41	$2.2 \times 10^{-2}$	$3.7 \times 10^{-1}$	$2.7 \times 10^{-2}$	13.7	—
	200	39	$7.2 \times 10^{-5}$	$1.0 \times 10^{-1}$	$4.7 \times 10^{-2}$	2.1	—
	300	13		$7.5 \times 10^{-4}$	$3.7 \times 10^{-3}$	—	4.9
PE–polyaniline	100	27	$2.9 \times 10^{-2}$	$5.4 \times 10^{-2}$	$3.9 \times 10^{-2}$	1.4	—
	200	42	$2.3 \times 10^{-2}$	$2.4 \times 10^{-1}$	$1.6 \times 10^{-1}$	1.5	—
PE–polyacetylene	200	8	$(0.2-1.4) \times 10^{-2}$	$(0.9-4.4) \times 10^{-2}$	$(0.9-1.3) \times 10^{-1}$	—	3–10

The studies were carried out to develop approaches for obtaining polymer blends where the second polymer introduced into the crazed polymer matrix had a high electrical conductivity [37–39]. Methodologically, the approaches described above were used in these studies. Polymer films (HDPE and PET) were crazed; then, the corresponding monomers (acetylene and aniline) were introduced into the nanoporous structure formed in drawing. The subsequent in situ polymerization of the introduced monomers and the doping of the resulting products yielded a number of promising materials, which successfully combined the high conductivity characteristic of polyacetylene and polyaniline with the good mechanical properties characteristic of HDPE and PET.

For the blends with conducting polymers, the characterization of their bulk and surface conductivity was carried out. Considering the specifics of the structure of the blends based on crazed polymers and the possibility of molecular orientation of the conductive polymer in the blend, the specific surface conductivity of the films was evaluated in two directions: along the stretching axis of the polymer in the medium and in the perpendicular direction. The data on the composition of blends and their electrical conductivity depending on the tensile strain of the initial polymer are presented in Table 1.

It turned out that the introduction of even a relatively small quantity of polyacetylene (8 wt.%) into HDPE, followed by doping the polymer blend with iodine, increases the bulk conductivity by 14–16 orders of magnitude, that is, to  $(0.2-1.4) \times 10^{-2} \text{ Ohm}^{-1} \text{ cm}^{-1}$  [37]. This fact indicates that the structure of the resulting polymer blend provides a low percolation threshold for conductivity. The special feature of the structure of the blends of PE with polyacetylene is that, in the polymerization in the pores, the polymer introduced into the crazed matrix acquires a noticeable molecular orientation, which, as known [75], greatly increases its conductivity. As a result, the specific surface conductivity of the blends along the drawing axis exceeds several times the electrical conductivity measured in the perpendicular direction.

The attempts to introduce another conductive polymer, polyaniline, into crazed polymer matrices deformed by the mechanism of classical (drawing of PE) or delocalized (drawing of PET) crazing were also successful [38, 39]. The main results of this study are presented in Tables 1 and 2. The comparison of the mechanical properties of pure polymer matrices deformed by 100 and 200% and the corresponding blends based on them are given in Table 2. It is clearly seen that such important mechanical characteristics as modulus of elasticity and strength of the resulting blends are in the range of the corresponding characteristics for the pure matrix and, in some cases, even exceed them. At the same time, the resulting blends show excellent conductive characteristics that are close to the conductivity of pure polyaniline (Table 1). The bulk electrical conductivity ( $\sigma_v$ ) of both types of blends is very high, regardless of the type of polymer matrix and regardless of whether the polymer is deformed by the mechanism of conventional (drawing of PET) or delocalized (drawing of PE) crazing. The molecular orientation of polyaniline in the porous matrix, in contrast to polyacetylene, is virtually absent. At the same time, it follows from the data of Table 1 that the surface conductivity values in the direction of the drawing axis ( $\sigma_s^\parallel$ ) and in the normal direction ( $\sigma_s^\perp$ ) differ markedly from each other, particularly for the PET matrix deformed by the mechanism of classical crazing.

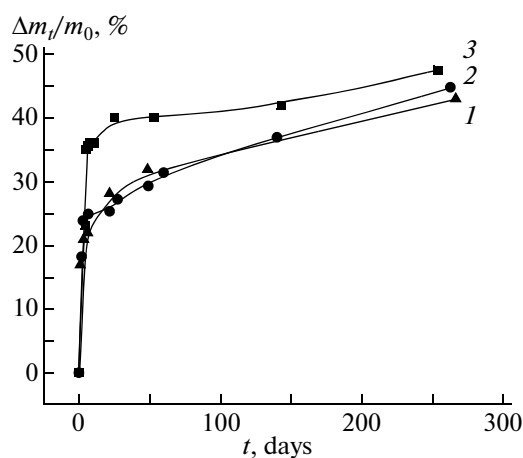


**Fig. 13.** Variation of the relative amount of the liquid medium of PEG 600 released from the PET samples deformed to various tensile strain: (1) 100, (2) 200, and (3) 300%.

For the small tensile strain of the polymer by the mechanism of classical crazing (50–200%), polyaniline is located in the crazes, separated by layers of undeformed dielectric polymer. In this connection, the electrical conductivity of the material in the direction perpendicular to the drawing axis is higher than along the drawing axis. With increasing tensile strain, the length of sections of the undeformed polymer between the crazes decreases, as shown schematically in Fig. 1. However, as a result of the collapse in the structure of the crazes, aggregates of coagulated fibrils begin to form, which far exceed their size at small tensile strain and are capable of increasing the resistance of the blends in a direction perpendicular to the drawing axis. This is reflected in the reduction of conductivity and the change in the character of its anisotropy to reversed. The electrical conductivity along the drawing axis of the polymer is higher than in the perpendicular direction.

Thus, the use of crazed polymer matrices for the in situ polymerization of conducting polymers can successfully combine in them high mechanical performance with optimal electrical conductivity. It follows from the presented data that the creation of new types of conductive polymer–polymer nanocomposites based on crazed polymer matrices can be very promising for applications.

#### 4.4. Prolonged Release of a High-Viscosity Component from the Structure of the Solvent-Crazed Polymer

The drawing of polymers in nonvolatile high-viscosity liquids, such as liquid oligomers, is of particular interest, since it enables one to observe the kinetics of migration of the environment from the pore volume and gives an idea about the stability of such systems and structural changes occurring over time in the crazed matrix [59]. For PET deformed in liquid oligomers PEG with molecular weight 400 and 600, a prolonged release of fluid trapped by the polymer over a long time (more than a year) was found. The release of PEG from the porous structure of crazed PET was assessed by changes in the weight of the deformed samples in time. The dependence characterizing the relative change in mass of PET films with PEG 600

**Table 2.** Mechanical characteristics of the nanoporous matrix of PET and PE and the blends with polyaniline based on them

Matrix or nanocomposite	$\lambda$ , %	C, %	$E$ , MPa	$\sigma_p$ , MPa	$\varepsilon_p$ , %	$E$ , MPa	$\sigma_p$ , MPa	$\varepsilon_p$ , %
			Along the drawing axis			Normal to the drawing axis		
PET	100	—	690	48	190	660	34	380
PET–polyaniline	100	40.8	1210	51	7	1000	17	4
PE	100	—	310	64	150	360	29	550
PE–polyaniline	100	26.6	730	64	180	650	31	550
PE	200	—	320	88	80	280	28	680
PE–polyaniline	200	42.2	930	86	90	870	30	5



in time is shown in Fig. 13. The starting points correspond to the quantity of PEG 600 captured by the polymer in the process of drawing and determined immediately after the release of the samples from the clamps of a stretching device. Then, the samples were left in the air under ambient humidity (relative humidity was approximately 30%) and wiped before each weighing to remove PEG transpired out on the film surface. Almost a year later, the system had not come into equilibrium, and the process of release of the liquid medium had not stopped. As seen from the data presented in Fig. 13, the curve characterizing the release of PEG from the blend consists of two parts. One can observe a sharp drop in the concentration of PEG 600 on the first day; later, a slowdown of this process occurs, and the next portion of the curve is characterized by a slow and sustained release, the intensity of which depends on the tensile strain and, as shown in [76], the ambient humidity.

Earlier, a similar release of high-viscosity liquids was found for PET deformed by the mechanism of crazing in highly viscous liquids such as ethylene glycol and solutions of ethylene glycol or glycerol in ethanol [77, 78]. The main reason for the release of liquids from the bulk of porous materials on the surface is capillary ascent. However, for the crazed polymer, the release of liquids also occurs for another reason related to the specifics of the nanoporous structure. The fact is that the structure of crazes is thermodynamically unstable, and after drawing it undergoes changes associated with the coagulation of individual fibrils. The result is a shrinkage of the polymer, and the liquid is squeezed out of the volume of the crazes.

This property of a system consisting of a dispersed polymer matrix and high-adsorption-active medium located in crazes may be of practical interest, since there is a need for materials with the controlled and sustained release of functional ingredients in medicine, cosmetics, the food industry, and agriculture [79–81].

In summary, we can conclude that the use of crazing of polymers in liquid media allows us to obtain a wide range of polymer–polymer blends of new types, with a high level of dispersion of components and new physical and mechanical properties.

#### ACKNOWLEDGMENTS

This work was supported by the Russian Foundation for Basic Research (project no. 09-03-00430-a), the Program “Leading Scientific Schools” (grant no. NSh-4371.2010.3), and the Russian Government (contracts nos. P1484 and 02.740.11.0143).

#### REFERENCES

1. Kuleznev, V.N., *Smesi polimerov* (Polymer Blends), Moscow: Khimiya, 1980.
2. Sperling, L., *Interpenetrating Polymer Networks and Related Materials*, New York: Plenum, 1981.
3. Donatelly, A.A., Sperling, L.H., and Thomas, D.A., *J. Appl. Polym. Sci.*, 1977, vol. 21, no. 5, p. 1189.
4. Yenwo, G.M., Sperling, R.H., Pulido, J., Manson, J.A., and Conde, A., *Polym. Eng. Sci.*, 1977, vol. 17, no. 4, p. 251.
5. Huelk, V., Thomas, D.A., and Sperling, R.H., *Macromolecules*, 1972, vol. 5, p. 340.
6. Allen, G., Bowden, L.J., Bundell, O.J., Jeffs, G.M., Vyvoda, J., and White, T., *Polymer*, 1973, vol. 14, p. 604.
7. Sionakidis, J., Sperling, L.H., and Thomas, D.A., *J. Appl. Polym. Sci.*, 1979, vol. 24, no. 5, p. 1179.
8. Yenwo, G.V., Manson, J.A., Pulido, J., Sperling, L.H., Conde, A., and Devia-Manjarres, N., *J. Appl. Polym. Sci.*, 1977, vol. 21, no. 7, p. 1531.
9. Siegfried, D.L., Sperling, R.H., and Manson, J.A., *J. Polym. Sci. Phys. Ed.*, 1978, vol. 16, p. 583.
10. Beginn, U., Fisher, E., Pieper, T., Mellinger, F., Kimmich, R., and Moller, M., *J. Polym. Sci., A*, 2000, vol. 38, p. 2041.
11. Tsutsui, H., Moriyama, M., Nakayama, D., Ishii, R., and Akashi, R., *Macromolecules*, 2006, vol. 39, no. 6, p. 2291.
12. Yong-Qing Xia, Tian-Ying Guo, Mou-Dao Song, Bang-Hua Zhang, and Bao-Long Zhang, *Biomacromolecules*, 2005, vol. 6, no. 5, p. 2601.
13. Gitsov, I., Chao Zhu, *J. Am. Chem. Soc.*, 2003, vol. 125, no. 37, p. 11228.
14. Kwok, A.Y., Qiao, G.G., and Solomon, D.H., *Chem. Mater.*, 2004, vol. 16, no. 26, p. 5650.
15. Dhara, D., Rathna, G.V.N., and Chatterji, P.R., *Langmuir*, 2000, vol. 16, no. 6, p. 2424.
16. Ogoshi, T., Itoh, H., Kim, K.-M., and Chujo, Y., *Macromolecules*, 2002, vol. 35, no. 2, p. 334.
17. Zecca, M., Biffis, A., Palma, G., Corvaja, C., Lora, S., Jrabek, K., and Corain, B., *Macromolecules*, 1996, vol. 29, no. 13, p. 4655.
18. Jackson, C.L., Bauer, B.J., Nakatani, A.I., and Barnes, J.D., *Chem. Mater.*, 1996, vol. 8, no. 3, p. 727.
19. Buyanov, A.L., Revel'skaya, L.G., Bobrova, N.V., and El'yashevich, G.K., *Vysokomol. Soedin., A*, 2006, vol. 48, no. 7, p. 1135 [*Polymer Sci., A* (Engl. Transl), vol. 48, no. 7, p. 738].

20. Nikitin, L.N., Gallyamov, M.O., Nikolaev, A.Yu., Said-Galiev, E.E., Khokhlov, A.R., Bukalov, S.S., Magdanurov, G.I., Volkov, V.V., Shtykova, E.V., Dembo, K.A., and El'yashevich, G.K., *Polymer Sci., A*, 2006, vol. 48, no. 8, p. 827.
21. Volynskii, A.L. and Bakeev, N.F., *Vysokodispersnoe orientirovannoe sostoyanie polimerov* (Highly Disperse Oriented State of Polymers), Moscow: Khimiya, 1985.
22. Volynskii, A.L. and Bakeev, N.F., *Solvent Crazing of Polymers*, Amsterdam: Elsevier, 1995.
23. Kambour, R.P., *J. Polym. Sci., Macromol. Rev.*, 1973, vol. 7, p. 1.
24. Narisawa, J. and Jee, A.F., *Mater. Sci. Technol.*, 1993, vol. 12, p. 701.
25. Yarysheva, L.M., Lukovkin, G.M., Volynskii, A.L., and Bakeev, N.F., in *Uspekhi kolloidnoi khimii i fiziko-khimicheskoi mekhaniki* (Advances in Colloid Chemistry and Physicochemical Mechanics), Shchukin, E.D., Ed., Moscow: Nauka, 1992.
26. Volynskii, A.L., *Priroda (Moscow, Russ. Fed.)*, 2006, no. 11, p. 11.
27. Volynskii, A.L., Mikushev, A.E., Yarysheva, L.M., and Bakeev, N.F., *Ross. Khim. Zh.*, 2005, vol. 49, no. 6, p. 118.
28. Arzhakova, O.V., Dolgova, A.A., Yarysheva, L.M., Chernov, I.V., Volynskii, A.L., and Bakeev, N.F., *Polymer Sci., A*, 2007, vol. 49, no. 8, p. 903.
29. Volynskii, A.L., Shitov, N.A., and Bakeev, N.F., *Vysokomol. Soedin., A*, 1981, vol. 23, no. 5, p. 978.
30. Yarysheva, L.M., Dolgova, A.A., Arzhakova, O.V., Volynskii, A.L., and Bakeev, N.F., *Vysokomol. Soedin., A*, 1993, vol. 35, no. 7, p. 913.
31. Volynskii, A.L., Chernov, I.V., Yarysheva, L.M., Lukovkin, G.M., and Bakeev, N.F., *Vysokomol. Soedin., A*, 1992, vol. 34, no. 2, p. 119.
32. Volynskii, A.L., Yarysheva, L.M., and Bakeev, N.F., *Polymer Sci., A*, 2001, vol. 43, no. 10, p. 1.
33. Yarysheva, L.M., Shmatok, E.A., Ukolova, E.M., Arzhakova, O.V., Lukovkin, G.M., Volynskii, A.L., and Bakeev, N.F., *Dokl. Akad. Nauk SSSR*, 1990, vol. 310, no. 2, p. 380.
34. Volynskii, A.L., Yarysheva, L.M., Shmatok, E.A., Ukolova, E.M., Lukovkin, G.M., and Bakeev, N.F., *Vysokomol. Soedin., A*, 1991, vol. 33, no. 5, p. 1004.
35. Volynskii, A.L., Yarysheva, L.M., and Bakeev, N.F., *Ross. Nanotekhnol.*, 2007, vol. 2, nos. 3–4, p. 58.
36. Sinevich, E.A., Prazdnichnyi, A.M., Bruk, M.A., Isaeva, G.G., Teleshchov, E.N., and Bakeev, N.F., *Vysokomol. Soedin., A*, 1991, vol. 33, no. 7, p. 1518.
37. Yarysheva, L.M., Saifullina, S.A., Rozova, E.A., Sizov, A.I., Bulychev, B.M., Volynskii, A.L., and Bakeev, N.F., *Vysokomol. Soedin., A*, 1994, vol. 36, no. 2, p. 363.
38. Saifullina, S.A., Yarysheva, L.M., Volkov, A.V., Volynskii, A.L., and Bakeev, N.F., *Polymer Sci., A*, 1996, vol. 38, no. 7, p. 754.
39. Saifullina, S.A., Yarysheva, L.M., Volynskii, A.L., and Bakeev, N.F., *Polymer Sci., A*, 1997, vol. 39, no. 3, p. 298.
40. Lipatov, Yu.S. and Sergeeva, L.M., *Vzaimopronikayushchie polimernye setki* (Interpenetrating Polymer Networks), Kiev: Naukova Dumka, 1979.
41. Tomas, D. and Sperling, L.H., in *Polymer Blends*, Paul, D. and Newman, C., Eds., New York: Academic, 1979, vol. 2, p. 5.
42. Efimov, A.V., Bondarev, V.V., Kozlov, P.V., and Bakeev, N.F., *Vysokomol. Soedin., A*, 1982, vol. 24, no. 8, p. 1690.
43. Volynskii, A.L., Shtanchaev, A.Sh., and Bakeev, N.F., *Vysokomol. Soedin., A*, 1984, vol. 26, no. 11, p. 2374.
44. Widmaier, J.H. and Sperling, L.H., *Macromolecules*, 1982, vol. 15, no. 2, p. 625.
45. Widmaier, J.M. and Sperling, L.H., *J. Appl. Polym. Sci.*, 1982, vol. 27, no. 12, p. 3513.
46. Frisch, H.L., Frisch, K.C., and Klempner, D., *Pure Appl. Chem.*, 1981, vol. 53, no. 8, p. 1557.
47. Heikens, D. and Barentsen, W.M., *Polymer*, 1977, vol. 18, no. 1, p. 69.
48. Sjoerdsma, S.D., Dalmolen, J., Bleijenberg, A.S., and Heikens, D., *Polymer*, 1980, vol. 21, no. 12, p. 1469.
49. Heikens, D., *Kern. Ind.*, 1982, vol. 31, no. 4, p. 165.
50. Donatelly, A.A., Sperling, L.H., and Thomas, D.A., *Macromolecules*, 1976, vol. 9, no. 4, p. 671.
51. Volynskii, A.L., Shtanchaev, A.Sh., and Bakeev, N.F., *Vysokomol. Soedin., A*, 1984, vol. 26, p. 1842.
52. Volynskii, A.L., Shtanchaev, A.Sh., Zanegin, V.D., Gerasimov, V.I., and Bakeev, N.F., *Vysokomol. Soedin., A*, 1985, vol. 27, p. 831.
53. Volynskii, A.L., Lopatina, L.I., and Bakeev, N.F., *Vysokomol. Soedin., A*, 1986, vol. 28, no. 2, p. 398.
54. Volynskii, A.L., Lopatina, L.I., Yarysheva, L.M., and Bakeev, N.F., *Polymer Sci., A*, 1997, vol. 39, no. 7, p. 778.
55. Volynskii, A.L. and Bakeev, N.F., *Advances in Interpenetrating Polymer Networks*, Klempner, D. and Frisch, K.C., Eds., Lancaster, Pennsylvania: Technomic, 1991, vol. 3, p. 53.
56. Volynskii, A.L., Lopatina, L.I., Yarysheva, L.M., and Bakeev, N.F., *Polymer Sci., A*, 1998, vol. 40, no. 2, p. 189.
57. Shtanchaev, A.Sh., Sergeev, V.G., Baranovskii, V.Yu., Lukovkin, G.M., Volynskii, A.L., Bakeev, N.F., and Kabanov, V.A., *Vysokomol. Soedin., A*, 1983, vol. 25, no. 9, p. 642.

58. Bykova, I.V., Prazdnikova, I.Yu., Bruk, M.A., Isaeva, G.G., Bakeev, N.F., and Teleshov, E.N., *Vysokomol. Soedin., B*, 1989, vol. 31, no. 1, p. 67.
59. Rukhlya, E.G., Arzhakova, O.V., Yarysheva, L.M., Volynskii, A.L., and Bakeev, N.F., *Polymer Sci., B*, 2007, vol. 49, nos. 5–6, p. 118.
60. Yarysheva, L.M., Rukhlya, E.G., Volynskii, A.L., and Bakeev, N.F., *Perspekt. Mater.*, 2008, no. 6 (2), p. 203.
61. Rukhlya, E.G., Yarysheva, L.M., Volynskii, A.L., and Bakeev, N.F., *Polymer Sci., A*, 2010, vol. 52, no. 6, p. 614.
62. Rukhlya, E.G., Yarysheva, L.M., Volynskii, A.L., and Bakeev, N.F., *Polymer Sci., B*, 2007, vol. 49, nos. 9–10, p. 245].
63. Rukhlya, E.G., Arzhakova, O.V., Dolgova, A.A., Yarysheva, L.M., Volynskii, A.L., and Bakeev, N.F., *Int. J. Polym. Anal. Charact.*, 2007, vol. 12, no. 1, p. 65.
64. Forrest, J.A., *Eur. Phys. J., E*, 2002, vol. 8, p. 261.
65. Volynskii, A.L. and Bakeev, N.F., *Polymer Sci., B*, 2003, vol. 45, nos. 7–8, p. 195.
66. Forrest, J.A. and Dalnoki-Veress, K., *Adv. Colloid Interface Sci.*, 2001, vol. 94, p. 167.
67. Volynskii, A.L., Shtanchaev, A.Sh., and Bakeev, N.F., *Vysokomol. Soedin., A*, 1984, vol. 26, no. 11, p. 2445.
68. Reitlinger, S.A., *Pronitsaemost' polimernykh materialov* (Permeability of Polymer Materials), Moscow: Khimiya, 1974.
69. Volynskii, A.L., Barvinskii, I.A., Lopatina, L.I., Volkov, A.V., and Bakeev, N.F., *Vysokomol. Soedin., A*, 1987, vol. 29, no. 7, p. 1382.
70. Volynskii, A.L., Lopatina, L.I., Arzhakov, M.S., and Bakeev, N.F., *Vysokomol. Soedin., A*, 1987, vol. 29, no. 4, p. 823.
71. Kargin, V.A., Gatovskaya, T.V., Pavlyuchenko, G.M., and Berestnev, V.A., *Dokl. Akad. Nauk SSSR*, 1962, vol. 143, no. 3, p. 590.
72. Kargin, V.A. and Usmanov, X.U., *Zh. Fiz. Khim.*, 1954, vol. 28, no. 2, p. 224.
73. Shchukin, E.D., Pertsov, A.V., and Amelina, E.A., *Kolloidnaya khimiya* (Colloid Chemistry), Moscow: Mosk. Gos. Univ., 1982.
74. Pertsov, A.V., in *Fiziko-khimicheskaya mekhanika i liofil'nost' dispersnykh sistem* (Physicochemical Mechanics and Liophilicity of Disperse Systems), Kiev: Naukova dumka, 1981, no. 13, p. 35.
75. *Conducting Polymers: Special Applications*, Alcacer, L., Ed., Dordrecht: Reidel, 1987.
76. Yarysheva, A.Yu., Polyanskaya, V.V., Rukhlya, E.G., Dement'ev, A.I., Volynskii, A.L., and Bakeev, N.F., *Colloid J.*, (in press).
77. Volynskii, A.L., Arzhakov, M.S., Karachevtseva, I.S., and Bakeev, N.F., *Vysokomol. Soedin., A*, 1994, vol. 36, no. 1, p. 85.
78. Yarysheva, L.M., Karachevtseva, I.S., Volynskii, A.L., and Bakeev, N.F., *Vysokomolek. Soedin., A*, 1995, vol. 37, no. 10, p. 1699.
79. Madene, A., Jacquot, M., Scher, J., and Desobry, S., *Int. J. Food Sci. Technol.*, 2006, no. 41, p. 1.
80. Allen, C., Maysinger, D., and Eisenberg, A., *Colloid Surf., B*, 1999, no. 16, p. 3.
81. Kwon, G.S. and Okano, T., *Adv. Drug Delivery. Rev.*, 1996, no. 21, p. 107.